Plateau Behavior in the Chiral Luttinger Liquid Exponent

A. M. Chang,[1,2] M. K. Wu,[2] C. C. Chi,[2] L. N. Pfeiffer,[3] and K. W. West[3]
[1]*Department of Physics, Purdue University, West Lafayette, Indiana 47907*
[2]*National Tsing-Hua University, 101 Kuang-Fu Road, Section 2, Hsin-Chu, Taiwan, Republic of China*
[3]*Bell Laboratories, Lucent Technologies, 700 Mountain Avenue, Murray Hill, New Jersey 07974*
(Received 16 June 1999)

The current-voltage power law exponent, α, for electron tunneling into chiral Luttinger liquids at the fractional quantum Hall edge is found to exhibit a *plateaulike structure* at α close to 3 as the filling factor, ν, is varied. The presence of a plateau near $\alpha = 3$ strongly suggests a fundamental connection between α and the structure of the underlying quantum ground states associated with the robust incompressible $\nu = 1/3$ Hall fluid. However, the position in the inverse filling factor where the plateau occurs can vary between samples and appears shifted to values higher than expected from theory.

DOI: 10.1103/PhysRevLett.86.143 PACS numbers: 71.10.Pm, 72.20.My, 73.40.Lq, 73.40.Hm

The low energy properties of conventional metals are well described by the Fermi-liquid picture when electron interaction is taken into account wherein long-lived, Fermionic quasiparticles (holes) comprise the low energy excitations as the energy approaches zero. In contrast, non-Fermi-liquid metallic systems are often distinguished by the *absence* of a single particle pole in the single particle spectral function replaced instead by power law dependences yielding a power law density of states for the tunneling of electrons and a suppression of tunneling at zero energy. The chiral Luttinger liquid (CLL) represents an extremely clean example of a non-Fermi liquid [1–4], resulting from the quasi-one-dimensionality and inherent strong correlations. Deriving its existence at the edge of the fractional quantum Hall (FQH) fluid, the CLL contains phononlike gapless excitations [1,2,5–11] and has been demonstrated to possess the Hallmark power law tunneling density of states observable in tunneling current-voltage (I-V) characteristics [1–4,6,8] in novel cleaved-edge overgrowth devices [12]. The observed power laws are of extraordinary quality and can span $4\frac{1}{2}$ decades in current and $1\frac{1}{2}$ decades in excitation voltage, a dynamic range far surpassing other promising Luttinger liquid systems such as carbon nanotubes [13,14], quasi-1D organic salts [15,16], or blue bronze conductors [17,18]. Furthermore, it is found that the power law behavior is not restricted to incompressible FQH fluids at special rational filling factors and is in fact present for general filling factors with the exponent, α, varying roughly as $1/\nu$ for $1/\nu > 1.3$ [3,4]. The observed behavior has presented a puzzle. For the incompressible $\nu = 1/3$ FHQ fluid, the low energy edge excitations are decoupled from the bulk excitations which contain a gap; thus the edge constitutes a truly one-dimensional system which theory predicts to be a CLL with a tunneling exponent of exactly 3 [1,2,5,6]. In contrast, at intermediate filling factors between incompressible Hall fluids, e.g., at the $\nu = 1/2$ compressible composite Fermion fluid, the existence of a power law I-V was not fully anticipated [3]. At present, while a hierarchical picture of incompressible fluids is able to produce power law behavior at a set of rational filling fractions [2], and a recent theory based on the composite Fermion picture predicts power laws at continuous values of $1/\nu$ [19] (more precisely Hall resistivity, ρ_{xy}), the predicted steplike plateau features in α stand in contrast to the featureless linear behavior of the experiment. These theories are based directly on our understanding of the relation between the edge mode structure and the topological characterization of FQH states, as well as the intermixing of copropagating and counterpropagating edge modes into charged and neutral varieties. Two major issues arise. First, the absence of plateaus for $1/\nu > 1.3$ is difficult to reconcile with current understanding even without accounting for the finite width of quantized Hall plateaus. Second, the lack of a plateau near bulk filling, $\nu = 1/3$ ($1/\nu = 3$), despite a plateau in ρ_{xy} indicates that the edge tunneling characteristic is not solely dictated by the bulk Hall resistivity, again in contradiction to expectation. This absence of structure has even been invoked by some workers as evidence that the existence of CLL behavior is not conclusive [13,20,21]. Because the $\nu = 1/3$ FQH fluid possesses the largest gap and is robust, evidence for plateauing in the exponent is of critical importance.

In this Letter we report the clear observation of a plateau feature for the α versus $1/\nu$ dependence with an α value close to 3. Our results obtained in two sets of samples are based on careful analysis of I-V tunneling data with precise fitting to the theoretical I-V dependence due to Chamon and Fradkin [22], followed by a statistical F-test for the χ^2 of the α versus $1/\nu$ fits *to establish the presence of a plateau feature with a confidence level exceeding 99% while rejecting a simple linear dependence*. Characterizing the α versus $1/\nu$ plot by the slope, $S \equiv d\alpha/d(1/\nu)$, in the first set of samples S exhibits an abrupt change from 1.15 ± 0.3, reflecting a roughly $\alpha \sim 1/\nu$ dependence, to 0.15 ± 0.15 as $1/\nu$ increases beyond 2.76, constituting a reduction of more than a factor of 7 in S. This plateau region of reduced slope extends from $1/\nu = 2.76$ to 3.33 before reverting to a value of $\sim$1.05 above $1/\nu = 3.33$. Similarly, in a second set, S abruptly reduces from

0.33 ± 0.3 for $1/\nu < 4.12$ to -0.14 ± 0.18 for $4.12 < 1/\nu < 4.76$ before increasing rapidly, e.g., $S > 1.5$ for $1/\nu > 4.76$. In both sets of data the plateau region is centered about a value for α of 2.7, slightly below 3. Even though these values of $\alpha \sim 3$ are in good agreement with theory, the corresponding $1/\nu$ values vary between sets and are shifted substantially to the high side of the theoretically predicted position of between 2 and 3 in $\rho_{xy}/(h/e^2)$ [2,19]. Recent theories are attempting to address the origin of such discrepancies [23–28].

The tunneling experiments are performed on samples grown by the cleaved-edge-overgrowth technique [12,29]. Please see Refs. [3,4] for details. Samples 1 and 2 comprise the first sample set and possess an identical two-dimensional electron gas (2DEG) from the same wafer but differ in the subsequent cleaved-edge overgrowth. The 2DEG is of density 1.08×10^{11} cm^{-2} and mobility 3×10^6 cm^2/V s. Sample 3 has a 2DEG density of 0.61×10^{11} cm^{-2} and a mobility of 8×10^5 cm^2/V s. The $Al_{0.1}Ga_{0.9}As$ barrier thickness for samples 1, 2, and 3 are 90, 125, and 50 Å, respectively. Judging from the quantum Hall characteristics, these samples are of higher quality than those which previously exhibited $\alpha \sim 1/\nu$ behavior [4]. The n + GaAs is doped to $(1.4–2 \times 10^{18})$ cm^{-3} carrier density, yielding a chemical potential of 65–83 meV from the GaAs band bottom (70–88 meV from the impurity band bottom), while the chemical potential of the 2DEG is approximately 25 meV (15 meV) above band bottom for samples 1 and 2 (3). Charge redistribution can take place across the barrier due to this chemical potential imbalance.

In Fig. 1 we show the longitudinal and Hall resistances for the 2DEG in samples 1 and 3 at the respective temperatures of 195 and 50 mK. The $\nu = 1/3$ fractional quantum Hall effect occurs at 13.4 and 7.6 T, respectively. In Figs. 2–4 we presents log-log plots of the tunneling I-V characteristics between the 2DEG and the n + GaAs bulk metal (solid curves) for samples 1, 2, and 3, respectively, in a wide range of magnetic fields/filling factors in order to deduce the behavior of the power law exponent, α, as a function of $1/\nu$. Successive curves are shifted in the positive direction on the horizontal axis by 0.3 units (a factor of 2) for clarity, and curves for which a sufficient dynamic range is available to yield a meaningful exponent are included. The dashed curves represent best fits to data as described below. Ideally, an I-V curve consists of three regimes: (a) a low voltage bias regime with a linear I-V where the thermal energy, kT, dominates over the voltage bias energy, eV, $(eV \leq 2\pi kT)$ [1,2], (b) an intermediate voltage bias regime $(2\pi kT \leq eV \leq T_S)$ exhibiting the important power law I-V behavior [1,2,22], and (c) a high bias saturation regime $(eV > kT_S)$ in which I-V approaches linearity again and where the tunneling conductance saturates to the two-terminal conductance of the 2DEG as the tunnel barrier becomes transparent. Here T_S represents a cross-over temperature with kT_S the crossover energy above which saturation takes place [22]. In fact essentially all data for samples 1 and 3 exhibit this generic behavior while noting that the thermally dominated low voltage bias, linear regime (a) is visible only when it is above the noise floor ($\sim 4fA$). Aside from the traces for which the saturation region is not included, the only significant exceptions occur for sample 3 in a few traces at the largest $1/\nu$ values, where there is evidence of an additional parallel channel for tunneling when the conductance falls below $\sim 0.5 \times 10^{-8}$ S (R exceeds 2×10^8 Ω).

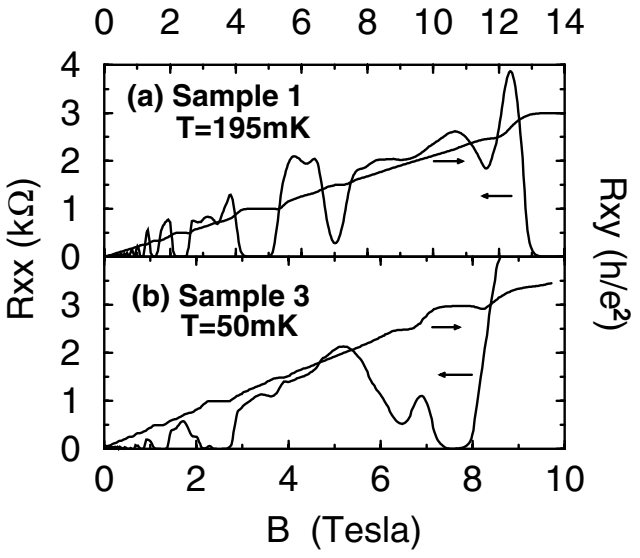

FIG. 1. Magnetic field traces of the longitudinal resistance (R_{xx}) and Hall resistance (R_{xy}), (a) for sample 1 at a temperature of 195 mK and (b) for sample 3 at 50 mK.

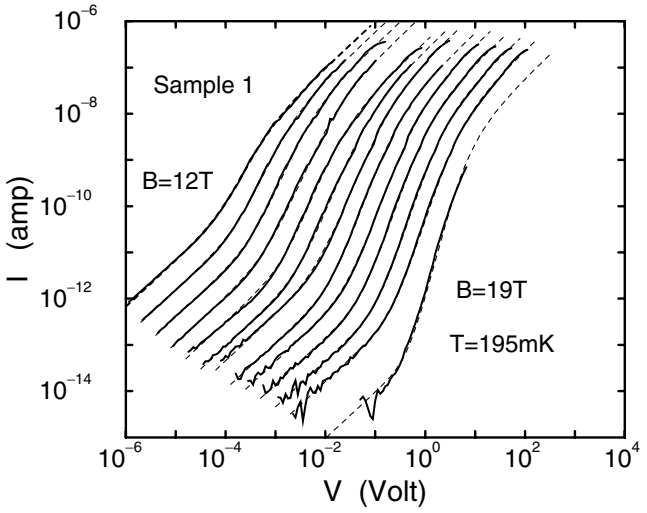

FIG. 2. Log-log plot of the I-V characteristics (solid lines) for electron tunneling from the FQH edge into the bulk doped n + GaAs in sample 1 at various magnetic fields from 12 to 19 T in steps of 0.5, 18, and 18.5 T excluded. Corresponding filling factors vary from 2.69 to 4.26. Dashed lines represent best fits to Eq. (1). Successive curves are shifted by 0.3 units (a factor of 2) in the x direction for clarity.

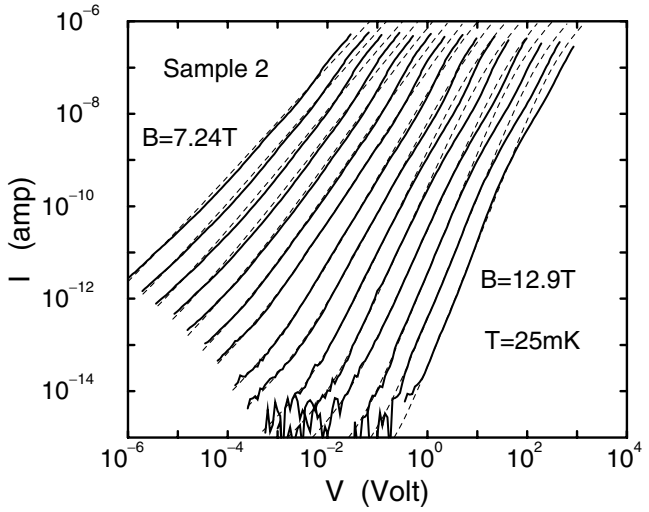

FIG. 3. Log-log plot of I-V characteristics (solid lines) for sample 2 at $B = 7.24$, 7.5, 7.76, 8.02, 8.28, 8.53, 8.79, 9.31, 9.83, 10.34, 10.86, 11.38, 11.9, 12.4, and 12.9 T ($1.611 < 1/\nu < 3$). Dashed lines represent best fits. Note x shifts for clarity.

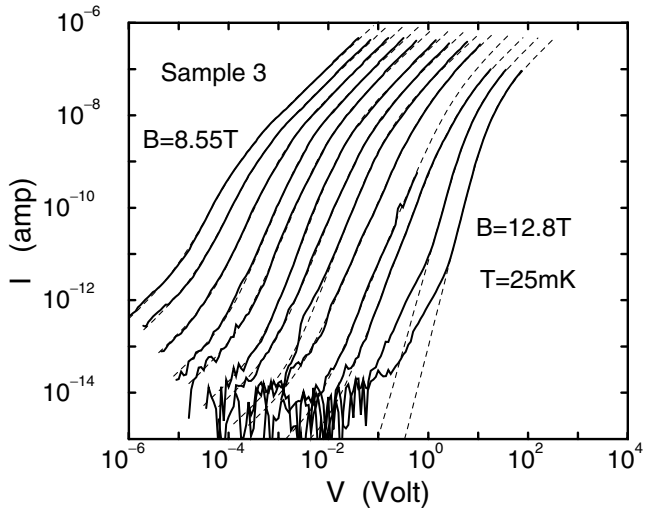

FIG. 4. Log-log plot of I-V characteristics (solid lines) for sample 3 at $B = 8.55$, 8.75, 9.15, 9.58, 10.0, 10.4, 10.8, 11.2, 11.6, 12.0, 12.2, 12.4, and 12.8 T ($3.605 < 1/\nu < 5.082$). Dashed lines represent best fits. Note x shifts for clarity.

In contrast sample 2 does not show an ideal saturation regime. This nonideality can arise from the opaqueness of the thicker tunnel barrier of 125 Å.

To establish the presence of a plateau feature in the exponent, α, we extract α in a systematic way by fitting the entire I-V range containing the three bias regimes to the Chamon-Fradkin expression for the tunnel current, I, at voltage, V, with the notation $\beta = \alpha - 1$, $r = \frac{2\pi T}{T_S}$:

$$I = \int_0^V \nu \frac{e^2}{h} \left(1 - \frac{e^{-\frac{1}{2}r^\beta}}{\left[\frac{(\frac{eV'}{rkT_S})^\beta}{\Gamma^2(\frac{\alpha+1}{2})}(1 - e^{-\frac{\beta}{2}r^\beta}) + 1 \right]^{\frac{\alpha}{\beta}}} \right) dV' \tag{1}$$

which represents a universal scaling formula for tunneling into a Luttinger liquid with exponent, α, in conjunction with the constraint that $V_a = V + IR_s$, where V_a is the voltage applied on the device across contacts and R_s is a 2DEG series resistance. Since the temperature is known, three parameters are needed: α, T_S, and a 2DEG series resistance R_s. The additional parameter R_s is needed to properly fit the saturation regime since at small filling factors (large $1/\nu$) the background from the longitudinal resistance of the 2DEG (R_{xx}) can be substantial (of order 100 $k\Omega$). For samples 1 and 3, a full fit over the entire range of I-V can be accomplished. The fitted I-V curves are plotted as dashed lines in Figs. 2 and 4. As evidenced by the nearly complete overlap of the fit and data in a majority of the traces, excellent fits are achieved. For sample 2, the absence of a true saturation regime precludes a full fit and the fitting is only performed within the low and intermediate bias regimes containing the linear and power law dependences. The affect on α is found to be minimal (<0.1) in traces which exhibit a sizable power law dynamic range occurring for $1/\nu > 2$. For $1/\nu \leq 2$ where $\alpha < 2$, nonlinearity arising from bias-induced reshaping of the tunnel barrier leads to distorted fits and systematic errors in α estimated to be less than 0.15. However, these $1/\nu \leq 2$ data points *turn out not to affect our conclusions*. In sample 3 the largest $1/\nu$, where $1/\nu > 4.9$, needs explanation. For these the intermediate bias regime contains two subregions of differing exponents with α_1 characterizing the lower portion crossing over to α_2 which characterizes the higher portion. The relevant exponent is α_2 for the following reasons. First of all, for traces with lower $1/\nu$, within noise, α is always either monotonically increasing or nearly flat with increasing $1/\nu$ and this trend is consistent with theoretical expectations. Second, the lower, α_1 subregion occurs at low conductances (below 0.5×10^{-8} S), where residual parallel tunneling channels can have an effect. In fact, at $1/\nu = 4.446$ corresponding to $B = 11.2$ T, excess conductance is already visible at bias voltages $10 \leq V \leq 100$ μV [note the displacement of a factor of $\log(2^7)$ for clarity], suggesting the presence of a parallel channel. In the traces in question, the low conductance regime is reached at higher values of voltage bias due to the large value of the exponent, α_2, and one may expect the effect of parallel channels to be more pronounced. Despite residual parallel conduction, the vast majority of traces are fully fitted by Eq. (1).

Figure 5 summarizes the fitting parameters α, T_S, and R_s deduced for the two sets of samples versus $1/\nu$. Results for samples 1 and 2 containing identical 2DEG are presented together. We focus our attention on α in panels (a) and (c). To establish unequivocally the presence of a plateau we first fit the data to curves containing (i) three line segments where the middle exhibits a reduced slope, (ii) two line segments, and (iii) single

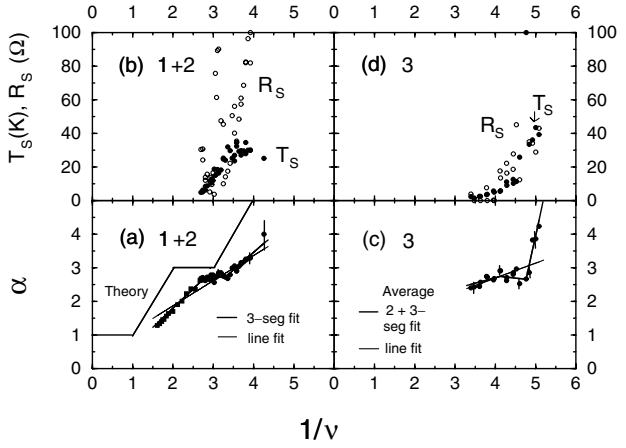

FIG. 5. The power law exponent, α, for samples 1 and 2, versus $1/\nu$, in (a) [for sample 3 in (c)]. Representative error bars are as shown, and solid curves are as labeled. The parameters T_S and R_s are summarized in panels (b) and (d).

straight lines, indexed by 3, 2, and 1, respectively. We next apply the statistical F-test on the random variable $F(n,m) = [(\chi_i^2 - \chi_j^2)/\chi_j^2]/[(df_i - df_j)/df_j]$ [30] to compare the χ^2's, where $(i,j) = 1,2,3$. Here $df_i = N - p_i$ represents the degree of freedom of the ith fit with N being the number of data points and p_i the number of fit parameters, while $n = df_i - df_j$ and $m = df_j$. When F exceeds the criterion for an integrated probability of 99% in the $F(n,m)$ distribution with n and m degrees of freedom, the jth fit is established while the ith fit is rejected with confidence exceeding 99%. For the first sample set the functional form with three line segments joined continuously (six parameters) is established while a simple linear fit (two parameters) is rejected (see Fig. 5a) as well as a two line (four parameter) fit. For the second set, both the three segment and two segment fits are viable while the single line fit is rejected (Fig. 5c). In both sets the plateau region occurs at $\alpha \sim 2.7$ with corresponding reduced slopes of 0.15 ± 0.15 and -0.14 ± 0.18. The respective F values for the two sets are 31.1 compared to the 99% confidence level criterion of $F(4,45) = 3.79$ ($N = 51$, $\chi_3^2 = 0.47$, $\chi_1^2 = 1.77$) and 17.9 compared to the average $[F(4,15) + F(2,17)]/2 = 5.5$ ($N = 21$, $\chi_3^2 = 0.45$, $\chi_2^2 = 0.66$, $\chi_1^2 = 2.26$). The result for the first set is robust even when the lowest seven points ($1/\nu \leq 2$) are removed. In terms of $1/\nu$ the plateau region occurs at $2.76 < 1/\nu < 3.33$ and $4.12 < 1/\nu < 4.76$, respectively. These positions are shifted to higher values compared to the theoretical prediction of $2 < 1/\nu < 3.3$ [2,19], taking into account the finite Hall plateau width. In the first sample set, the position corresponds well with the bulk $\nu = 1/3$ FQH plateau. On the other hand, *in the second set it is shifted substantially beyond the position of the $\nu = 1/3$ plateau.* At present it is not well understood how this shift occurs, although one possibility arises from edge reconstruction due to density gradients [25].

A. M. C. thanks Virginia Pang-Ying Yeh Chang for her contributions. He also acknowledges stimulating conversations with M. Fisher, E. Fradkin, B. Halperin, C. Kane, L. Levitov, and X.-G. Wen. Work at Purdue was supported by NSF Grant No. DMR-9801760. Work at Tsing-Hua University was supported by the Taiwan National Science Council.

[1] X. G. Wen, Phys. Rev. B **43**, 11 025 (1991); Phys. Rev. Lett. **64**, 2206 (1990); Phys. Rev B **44**, 5708 (1991); Int. J. Mod. Phys. B **6**, 1711 (1992).
[2] C. L. Kane and M. P. A. Fisher, Phys. Rev. B **46**, 15 233 (1992); Phys. Rev. Lett. **68**, 1220 (1992); Phys. Rev. B **51**, 13 449 (1995).
[3] A. M. Chang, L. N. Pfeiffer, and K. W. West, Phys. Rev. Lett. **77**, 2538 (1996); Physica (Amsterdam) **249B–251B**, 383 (1998).
[4] M. Grayson *et al.,* Phys. Rev. Lett. **80**, 1062 (1998).
[5] P. Fendley *et al.,* Phys. Rev. Lett. **74**, 3005 (1995).
[6] K. Moon *et al.,* Phys. Rev. Lett. **71**, 4381 (1993).
[7] K. Imura and N. Nagaosa, Phys. Rev. B **55**, 7690 (1977).
[8] W. J. Zheng and Yue Yu, Phys. Rev. Lett. **79**, 3242 (1997).
[9] J. M. Luttinger, J. Math. Phys. **15**, 609 (1963); S. Tomonaga, Prog. Theor. Phys. **5**, 544 (1950).
[10] F. D. M. Haldane, J. Phys. C **14**, 2585 (1981); Phys. Rev. Lett. **47**, 1840 (1981).
[11] U. Zülicke and A. H. MacDonald, Phys. Rev. B **54**, R8349 (1996).
[12] L. N. Pfeiffer *et al.,* Appl. Phys. Lett. **56**, 1697 (1990).
[13] M. Bockrath *et al.,* Nature (London) **397**, 598 (1999).
[14] Z. Yao *et al.,* Nature (London) **402**, 273 (1999).
[15] A. Schwartz *et al.,* Phys. Rev. B **58**, 1261 (1998).
[16] B. Dardel *et al.,* Europhys. Lett. **24**, 687 (1993).
[17] M. Sing *et al.,* Phys. Rev. B **59**, 5414 (1999).
[18] J. D. Denlinger *et al.,* Phys. Rev. Lett. **82**, 2540 (1999).
[19] A. V. Shytov *et al.,* Phys. Rev. Lett. **80**, 141 (1998).
[20] R. Egger, Phys. Rev. Lett. **83**, 5547 (1999).
[21] A. Altland *et al.,* Phys. Rev. Lett. **83**, 1203 (1999).
[22] C. Chamon and E. Fradkin, Phys. Rev. B **56**, 2012 (1997).
[23] S. Conti and G. Vignale, Physica (Amsterdam) **1E**, 101 (1997); J. Phys. Condens. Matter **10**, L779 (1998).
[24] U. Zuelicke and A. H. MacDonald, Physica (Amsterdam) **1E**, 105 (1997); Physica (Amsterdam) **3E**, 229 (1998).
[25] D. H. Lee and X.-G. Wen, cond-mat/9809160; K. Imura, cond-mat/9812400.
[26] A. Lopez and E. Fradkin, Phys. Rev. B **59**, 15 323 (1999); B. Skoric and A. Pruisken, Nucl. Phys. **B539**, 637 (1999).
[27] A. Alekseev, V. Cheianov, A. P. Dmitriev, and V. Yu. Kachorovskii, cond-mat/9904076.
[28] Yue Yu, Wenjun Zheng, and Zhongyuan Zhu, Phys. Rev. B **56**, 13 279 (1997); Yue Yu, cond-mat/9906123.
[29] M. Grayson *et al.,* Solid State Electron. **40**, 236 (1996).
[30] See, for example, C. Daniel and F. S. Wood, *Fitting Equations to Data; Computer Analysis of Multifactor Data* (Wiley-Interscience, New York, 1971, 1980).